ACS OMEGA

http://pubs.acs.org/journal/acsodf

Article

Application of Layered Double Hydroxides as a Slow-Release Phosphate Source: A Comparison of Hydroponic and Soil Systems

Abhinandan Singha Roy, Marinda de Beer, Sreejarani Kesavan Pillai, and Suprakas Sinha Ray*

Cite This: *ACS Omega* 2023, 8, 15017−15030

Read Online

ACCESS | Metrics & More | Article Recommendations | Supporting Information

ABSTRACT: The utilization of slow-release fertilizer materials capable of responding to their environment and releasing nutrient ions efficiently over a prolonged period is an emerging research area in agricultural materials sciences. In this study, two-dimensional layered materials were prepared to release phosphor ions (P) slowly into the soil as well as in the hydroponic system. Various P-intercalated layered double hydroxides (LDHs) (Mg/Al, Zn/Al, and Mg-Zn/Al-LDHs) with a molar ratio of 2:1 were synthesized using an ion-exchange method from corresponding LDHs containing NO_3^- ions within the layers. Sodium alginate (SA) was used to encapsulate P-intercalated Mg/Al-LDH to produce bionanocomposite beads (LB) to check the effect of the biopolymer matrix on the release characteristics. The prepared materials were characterized by XRD and FTIR to confirm the incorporation of P in LDHs. TGA, SEM, and elemental analysis were also performed to study the thermal decomposition pattern, surface morphology, and chemical composition of synthesized materials. The P-release experiments were conducted in a soil solution. The performance of the prepared materials was investigated in soil as well as in a hydroponic system for tomato plants under a controlled atmosphere of humidity, temperature, and light. The fertilization ability of the prepared materials was compared with that of a soluble P source (KH_2PO_4), commercial hydroponic fertilizer (Nutrifeed), and a commercial soil slow-release fertilizer (Wonder plant starter). The prepared materials demonstrated a slow release of P in the soil solution. P-intercalated LDHs were not very effective under hydroponic conditions; however, the LDHs were more effective in the soil system in terms of dry matter production and P content in dry matter. Furthermore, LDHs were able to increase the soil pH value over time.

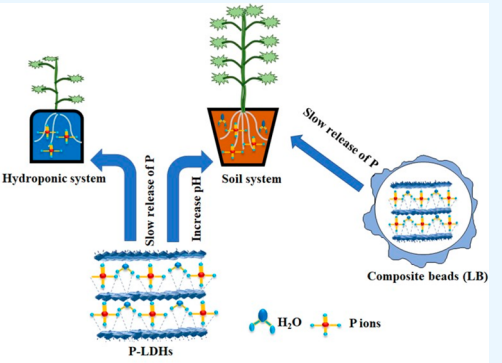

1. INTRODUCTION

Some crucial plant nutrients are responsible for plant growth and crop yield, such as phosphorus (P). Still, plant-available P exists only at minimal concentrations in the soil because of the very strong sorption or precipitation of the P anions.[1] In acidic soils, strong adsorption of the P ion occurs irreversibly, particularly in (oxy)hydroxides of Fe and Al. In contrast, P reacts with Ca^{2+} or Fe^{3+} in calcareous soils and produces a poorly soluble form.[2,3]

Globally, P is mainly used in the agricultural industry, employing around 80−90% of the extracted P worldwide.[4] However, plants can take up only 5−30% of the total P applied to the soils because of the low effectiveness of P fertilizer. The excess P in the soil is not available to plants due to immobilization by the precipitation of Fe^{3+} and Al^{3+}.[5,6] The excess or unused P can pollute streams or other surface water near agriculture fields by erosion and runoff of P from the soil. This can become a severe issue for aquatic life due to the excessive growth of algae resulting from eutrophication.[7] The primary origin of P is phosphate rocks, which are not a flow resource; for that reason, the use of P in agriculture should be optimized. To increase P fertilizer effectiveness and prevent nutrient losses, we need to develop a new method to recycle P and make it more readily available to plants. To optimize the P uses in agriculture, many new P-fertilizer methods have been introduced, such as rock phosphate with less solubility,[8,9] the use of an alternate P origin to prepare P fertilizer,[10,11] and polymer-coated P fertilizer,[12,13] while nowadays slow-release fertilizers (SRFs) are mainly used because of their high potential for agricultural field conditioning.[14,15]

Fertilizers with slow-release functionality are expected to release the nutrients over a longer time at a rate that meets their nutrient demand, unlike conventional fertilizers that quickly dissolve in the soil and provide nutrients in a relatively short time.[16] SRFs enhance nutrient use efficiency and decrease the frequency of application required. Furthermore, proper fertilizer management through SRFs circumvents nutrient losses to the environment, decreases soil contami-

Received: December 9, 2022
Accepted: March 14, 2023
Published: April 20, 2023

Table 1. List of Cations, Anions, Molar Ratio of Cations, and Number of Moles Used for the Synthesis of the NO_3^- Form of LDHs

			molar ratio	moles		
LDH	cations	anions	M^{2+}/M^{3+}	Mg^{2+}	Zn^{2+}	Al^{3+}
Mg/Al-LDH	Mg^{2+}, Al^{3+}	NO_3^-	2:1	0.03		0.015
Zn/Al-LDH	Zn^{2+}, Al^{3+}	NO_3^-	2:1		0.03	0.015
Mg-Zn/Al-LDH	Mg^{2+}, Zn^{2+}, Al^{3+}	NO_3^-	1:1:1	0.015	0.015	0.015

nation, and prevents nutrient contamination in water and the atmosphere. However, the development of SRFs with multifunctionality and environmental compatibility is still a great challenge in agricultural material technologies.[17] The disadvantages include high cost, low efficacy, and environmental concerns. The SRFs are typically manufactured by coating the conventional soluble fertilizers with low-cost fossil-fuel-based synthetic polymers, which are not biodegradable.[18] Hence it is crucial to design economically viable and environmentally friendly fertilizer materials and inert encapsulating matrixes that can function at the optimum level.

The use of synthetic anionic nanolayered double hydroxides (LDHs) in agriculture as SRFs is gaining a lot of attention recently due to the multifunctionality of the material. LDHs are two-dimensional layered nanomaterials structurally similar to brucite $Mg(OH)_2$, with some divalent metal ions replaced with trivalent metal ions. These nano-LDHs have the chemical formula $[M^{2+}_{1-x}M^{3+}_{x}(OH_2)]^{x+}(A^{n-})_{x/n}{\cdot}yH_2O$ [where M^{2+} is a divalent metal ion (e.g., Mg^{2+}, Zn^{2+}, or Mn^{2+}); M^{3+} is a trivalent metal ions (e.g., Al^{3+}, Fe^{3+}, or Cr^{3+}); A^{n-} is an intercalated anion (e.g., NO_3^-, CO_3^{2-}, or Cl^-), and x is the fractional aluminum substitution in the layers.[19] LDHs are ecofriendly and cost-effective materials with slow anion-release properties due to their ion-exchange properties. LDHs are flexible layered structures with a positive surface charge that can accommodate various anions in the interlayer space. They also offer a relatively high surface area, crystalline structure, water resistance, and biocompatibility.[20] Some studies also reported the prospects of LDHs as sources of macro- and micronutrients.[20−22] Due to their high anion-exchange capacity, LDHs are considered to be suitable sorbents for various types of anions, including agricultural nutrients. The anion adsorption by LDHs occurs via various mechanisms such as electrostatic attraction (on the surface), anion exchange with interlayer anions, and surface complexation.[23] The flexible nature of the electrostatic and interlayer anion bonding in LDHs makes these materials particularly interesting as sources of anionic nutrients for plant uptake since counteranions from the soil solution (e.g., carbonate) can slowly exchange with the anionic nutrient in the LDHs. LDHs can quickly release the nutrient ions from the external surfaces; thereafter, the intercalated nutrient ions release slowly. A couple of research data points already show that LDHs release P much slower than other commercial fertilizers.[14,24]

In neutral soils, the LDHs release P slowly because of an ion-exchange reaction between the loaded phosphor ions and the carbonate anions from the soil.[25,26] This ion exchange could be associated with P release in acidic soil because of LDH dissolution. Thus, LDHs may release P in response to a certain environmental condition, which the plant might use later to overcome a P deficiency. The simultaneous release of hydroxide ions from the lattice would be beneficial in neutralizing the acidity of the soil caused by excess agrochemicals.[27] Many works have demonstrated the synthesis and characterization of P-loaded LDHs and evaluated their slow-release properties using an aqueous or buffered medium.[28−30] The release rate of P depends on the intercalated P species; according to Woo et al.[27] and according to the report, monovalent $H_2PO_4^-$ was released more gradually than the other species. According to Koilraj et al.,[31] P-Ni/Al LDH demonstrated higher plant growth for green seaweed *Ulva lactuca* compared to the soluble P source. Everaert et al.[24] pointed out that although the agronomic effectiveness of LDHs is lower than that of conventional soluble P fertilizers, they can add tremendous value in an agricultural environment with an excess nutrient problem to regulate the P cycle. The rate of nutrient release from LDHs depends on the soil or water pH; at a lower pH, the release rate increases, thus affecting the structural stability of LDHs.[32] The structural stability can rapidly decrease when LDH is applied in a powder form in an acidic medium, which can hamper the slow-release behavior.[33] Encapsulation of LDHs using natural polysaccharides such as alginate can be an alternate strategy to prevent direct contact of LDH with acidic soil while improving the slow-release properties. Alginate is a natural biodegradable polymer that absorbs and holds rainwater or irrigation water, reducing water loss through groundwater recharging.[34,35] Moreover, the slow-release properties of LDHs in both aqueous and soil environments indicate their potential as a nutrient delivery system in hydroponics and for soil conditions. Many of the previous studies were limited to a single LDH material, where the conclusions on the efficacy of the material were based on the experiments under controlled conditions. The studies highlighting the applicability of different LDH materials in field trials for a particular crop with regard to nutrient bioavailability to the plant system and soil are limited. In this work, a comparative evaluation of structural and slow-release properties of binary, ternary, and biopolymer encapsulated LDHs, along with the analysis of the performance efficacy of the materials in solution and under crop conditions, is described. To the best of our knowledge, this study is the first to evaluate the effect of different LDHs and encapsulated LDHs on P usage efficiency with respect to the growth of tomato plants under soil and hydroponic farming conditions.

The work involved the synthesis and characterization of powdered Mg/Al, Zn/Al, and Mg-Zn/Al-LDHs containing P and the encapsulation of Mg/Al-LDH in an alginate matrix. The structural, morphological, and chemical characterization of the LDHs was systematically carried out with a combination of diffraction, microscopic, and spectroscopic techniques. This was followed by release and plant growth experiments, comparing the efficiency of LDH materials and composite beads to that of commercial counterparts.

2. EXPERIMENTAL SECTION

2.1. Materials. Magnesium nitrate hexahydrate ($Mg(NO_3)_2{\cdot}6H_2O$, 98%), zinc nitrate hexahydrate ($Zn(NO_3)_2{\cdot}6H_2O$, 98%), and aluminum nitrate nonahydrate ($Al(NO_3)_3{\cdot}$

https://doi.org/10.1021/acsomega.2c07862
ACS Omega 2023, 8, 15017−15030

$9H_2O$, 98%) were obtained from Sigma-Aldrich (South Africa). Sodium hydroxide and sodium nitrate were obtained from Minema Chemicals (South Africa). Potassium dihydrogen orthophosphate (KH_2PO_4) and sodium alginate were obtained from SRL (Sisco Research Laboratories, India). Ultrapure water obtained by a Milli-Q system (Merck Millipore, Merck, South Africa) was used in all experimental methods. The commercial fertilizers, namely, Nutrifeed (a water-soluble hydroponics nutrient) and Wonder Plant Starter (PS) (a slow-release granular fertilizer), were purchased from Chamberlains Store, Pretoria, South Africa.

2.2. Synthesis of NO_3^--LDHs (N-LDHs). The NO_3^- forms of Mg/Al-LDH, Zn/Al-LDH, and Mg-Zn/Al-LDH (N-LDHs) were synthesized by coprecipitation at low supersaturation. In a typical procedure, appropriate amounts of $Mg(NO_3)_2{\cdot}6H_2O$ or $Zn(NO_3)_2{\cdot}6H_2O$ and $Al(NO_3)_3{\cdot}9H_2O$ were weighed (M^{2+}/M^{3+} molar ratio 2:1, Table 1) and dissolved with hot decarbonated water (100 mL). The mixed metal solution was then added dropwise to a 500 mL beaker containing 100 mL of a 1.0 M sodium nitrate solution under vigorous stirring. The reaction was performed in a nitrogen gas atmosphere to prevent the formation of carbonate in the solution. Throughout the synthesis, the pH of the suspension was kept between 9.0 and 10.0 by adding appropriate amounts of 1.0 M sodium hydroxide (NaOH) dropwise to the mixture. The white suspension was allowed to age in the synthesis mixture for 18 h at room temperature (25 °C) in a closed round-bottomed flask. The material was recovered by centrifugation, washed several times with ultrapure water, and dried under vacuum at 60 °C. The Mg/Al-LDH material was ground and sieved through a 75 μm mesh sieve. Final powder samples were kept in a sealed aluminum foil bag for further analysis and experiments. Zn/Al-LDH and Mg-Zn/Al-LDHs were synthesized using a similar procedure by varying the salt precursors.

2.3. Synthesis of P-LDHs. The preparation of P-intercalated LDHs (P-LDHs) through the coprecipitation method is difficult due to the competitive formation of metal phosphates instead of LDH. In addition, P ions can resist the changes in the pH value of the solvent on the addition of a small amount of an acid or a base.[36] Hence, P-LDH was synthesized in two steps: in the first step, NO_3^--intercalated LDH was prepared by the coprecipitation method as described above, and in the second step, the ion exchange method was used to intercalate the P ions into the prepared NO_3^--LDH.

For this step, 2.0 g of NO_3^--intercalated Mg/Al-LDH and Mg-Zn/Al LDH was suspended in 200 mL of a 1.0 M KH_2PO_4 solution. Before the addition of the LDHs, the pH of the KH_2PO_4 solution was adjusted to 7 using a 0.1 M sodium hydroxide solution. The white suspension was stirred in a nitrogen atmosphere for 24 h at 70 °C. At the end of the exchange reaction, the material was recovered by centrifugation, washed several times with ultrapure water, and dried under vacuum at 60 °C.

The same procedure was followed for the Zn/Al-LDH exchange reaction, except that 2.0 g of the LDH was suspended in 0.3 M KH_2PO_4 solution instead of 1.0 M KH_2PO_4 solution. This was done because at higher P-ion concentrations, the XRD results showed the preferential formation of ZnO and $Zn(OH)_2$ phases instead of LDHs, and the results were in agreement with Bernardo et al.[37] (Figure S1).

2.4. Synthesis of LDH Beads. LDH-alginate beads (LB) were prepared by entrapping the powdered form of P-Mg/Al-LDH in a sodium alginate (SA) matrix. The alginate solution was prepared by mixing sodium alginate (0.2 g) with ultrapure water (30 mL). After 30 min of constant stirring, 1 g of the P-Mg/Al-LDH material was added to the alginate solution and agitated further at room temperature for 2 h in a closed environment to ensure homogeneity. This alginate/P-Mg/Al-LDH suspension was then added dropwise to 100 mL of 0.3 M calcium nitrate ($Ca(NO_3)_2{\cdot}6H_2O$) solution to produce the beads. Prepared beads were washed with ultrapure water and dried in a freeze-dryer for 24 h.

2.5. Characterization. XRD spectra of the various LDHs (Mg/Al, Zn/Al, Mg-Zn/Al-LDH, LB, and SA) were obtained with a PANalytical X'Pert Pro X-ray diffractometer (Netherlands) using Cu Kα radiation (λ = 1.5406 Å) with a filament intensity of 40 mA and a voltage of 45 kV. Scans were conducted between 2θ = 0 and 40° at a scan speed of 2°/min and a scanning step of 0.02°. Infrared spectra were collected on an ATR FTIR spectrometer (PerkinElmer Spectrum 100 FTIR spectrometer, USA) from 4000 to 500 cm^{-1} through eight scans at 4 cm^{-1} resolution. A thermogravimetric analyzer (TA Instruments TGA5500 Discovery series, USA) was used at a heating rate of 10 °C/min to measure the thermal decomposition patterns of various LDHs. The surface morphology of the various LDHs and LB was captured with a scanning electron microscope (JEOL JSM-7500F field emission electron microscope, Japan) with an accelerating voltage of 3.0 kV and an emission current of 10 μA. To quantify metal concentrations of the P-LDHs, 0.10 g of the samples was digested in 0.1 M HCl solution. From the extracts obtained, the amounts of Mg, Zn, and Al were determined by inductively coupled plasma optical emission spectrometry (PerkinElmer ICP Optima 2000 DV). The number of P ions in P-LDHs was determined by ion chromatography (Dionex ICS-5000$^+$ SP, Thermo Scientific, USA).

2.5.1. Soil Characterization. The soil used in this study for the plant growth experiments was collected from the surface layer (0−20 cm) in the eastern region of Pretoria, South Africa. The measured characteristics of the soil are listed in Table 2.

Table 2. Physicochemical Properties of Soil

property	unit	value	method used
sand	%	56.34 ± 0.89	Bouyoucos[38]
silt	%	33.21 ± 0.77	Bouyoucos[38]
clay	%	11.44 ± 0.85	Bouyoucos[38]
pH		6.56 ± 0.07	Okalebo et al.[39]
cation exchange capacity (CEC)	mol/kg	10.80 ± 0.53	Pleysier and Juo[40]
available P	mg/kg	18.78 ± 0.77	Turrión et al.[41]
organic matter	%	2.05 ± 0.32	Schutte et al.[42]
water-holding capacity	%	32.26 ± 0.88	Okalebo et al.[39]

2.6. P Release from P-LDHs. The release profiles of P from P-LDHs were obtained in soil solutions. To prepare the soil solution, 20 g of soil was mixed with 400 mL of ultrapure water with constant stirring at 300 rpm using a mechanical stirrer. After 72 h of agitation, the solids were separated by centrifugation at 6000 rpm (30 min) in an ultracentrifuge (Nuve NF 800R). The final solution was collected and used as a soil solution for release studies. The measured pH of the soil solution was 6.5. All of the release studies were conducted at 25 °C.

https://doi.org/10.1021/acsomega.2c07862
ACS Omega 2023, 8, 15017−15030

The P release from P-LDHs and LDH beads (LB) was compared with the release from soluble PO_4 sources (KH_2PO_4 and Nutrifeed, commercially available water-soluble hydroponics nutrient) and a sustained release granular fertilizer (PS commercially available sustained-release fertilizer). In a typical experiment, the amount of P-LDH equivalent to 5 mg of P was added to the soil solution in a chemical laboratory reagent bottle (100 mL). The bottle was placed in a constant-temperature water bath at 25 ± 1 °C and was shaken at 100 rpm. Samples (5 mL) were collected after 0.08, 0.17, 0.25, 0.5, 1, 2, 4, 8, 24, 48, 72, and 168 h. The removed sample was replaced with 5 mL of fresh soil solution to maintain a constant volume. The samples were filtered through a 45 μm (PVDF) syringe filter, and the filtrate was used to analyze the amount of P released from P-LDHs, LB, KH_2PO_4, Nutrifeed, and PS. All of the release experiments were conducted in triplicate, and average values were presented.

2.7. Tomato Plant Growth Experiments. *2.7.1. Tomato Plant Growth in a Hydroponic System.* The use of P-LDHs as suitable P fertilizers was screened by growing tomato plants under hydroponic conditions. P-LDH efficiency as a source of P for plant growth was compared with that of other soluble P sources, namely, KH_2PO_4 and Nutrifeed. For the hydroponic setup, 500 mL white buckets with lids were used with duct tape to cover the outer side of the buckets to prevent light from reaching the water solution. A hole was made in the middle of the lid to hold a 50 mm net pot. Rockwool cubes (RW) were used as a growing medium in the hydroponic system. Six tomato seeds were placed 1 cm below the top surface of the RW cubes which were moistened with ultrapure water. After 3 days at a temperature of 20 °C, the seeds germinated. The three visually "weaker" seedlings on each RW cube were removed, and only the three strongest or more healthy-looking seedlings were kept for growth experiments. RW cubes with seedlings were then transferred to the 50 mm net pots. The commercially available Nutrifeed fertilizer contains P as well as additional macro and micronutrients such as N, Mg, Cu, B, and Mn. To establish an equal amount of nutrients as available in Nutrifeed, a nutrient solution containing NH_4NO_3, $MgSO_4$, $CuSO_4$, H_3BO_3, and $MnSO_4$ was prepared. In each of the 500 mL buckets, 200 mL of the nutrient solution was added, except for the three buckets that were filled with 200 mL of Nutrifeed. Potassium chloride (KCl 5.36 mmol/L) solution was applied to the buckets treated with P-LDHs and Nutrifeed to maintain the same K doses as in the buckets treated with KH_2PO_4. The solution pH was adjusted to 6 using a potassium hydroxide solution. From each P source, namely, P-Mg/Al-LDH, P-Zn/Al-LDH, P-Mg-Zn/Al-LDH, KH_2PO_4, and Nutrifeed, the exact quantity of material was added to each bucket to give 150 mg/L P. The P sources were directly added to the 200 mL nutrient solutions in each bucket. As a control, an experiment without P but only nutrient solution was also performed.

The growth experiments were conducted in triplicate in a plant growth chamber. The chamber conditions were kept constant at a temperature of 23 °C, a humidity of 65%, and a light−dark cycle of 14 h of light and 10 h of dark.

2.7.2. Tomato Plant Growth in a Soil System. The soil collected from the surface layer (0−20 cm) in the eastern region of Pretoria, South Africa, was used for tomato plant growth. The soil was air-dried and sieved through a 2 mm sieve to determine the physicochemical properties (Table 2). The P fertilization efficiency and the P exchanged from P-LDH and P-LDH-beads were determined and compared with a soluble P source (KH_2PO_4) and commercial slow-release fertilizer PS by growing tomato plants in soil. For the soil experimental setup, 250 mL polystyrene cups with small holes on the bottom of the cups to drain the excess water were used. Cups were filled with 250 mL of soil. The exact quantity of P (150 mg·kg^{-1}) was applied in all of the cups from every P source (P-Mg/Al-LDH, P-Zn/Al-LDH, P-Mg-Zn/Al-LDH, LB, KH_2PO_4, and PS), and the P source was mixed with soil uniformly across the cups. An experiment without P was also carried out as a control. To establish an equal N dose of the nutrient source as for the cups treated with PS, NH_4NO_3 solution was applied to the cups treated with P-LDHs, LB, and KH_2PO_4. A smaller quantity of KCl solution was applied to the cups treated with P-LDH, LB, and PS to maintain the same K dose as for the cups treated with KH_2PO_4, and a nutrient solution of $MgSO_4$, $CuSO_4$, H_3BO_3, and $MnSO_4$ was further used in all of the cups. The water level was maintained at 70% by applying deionized water.

Tomato seeds were placed on paper towels, moistened with ultrapure water, and aged for 3 days to germinate the seeds at 20 °C. Four tomato seedlings were planted in each cup. The growth experiments were conducted in triplicate under the same conditions as in a hydroponics system in a plant growth chamber. The chamber conditions were kept constant at a temperature of 23 °C, a humidity of 65%, and a light−dark cycle of 14 h light and 10 h dark.

2.7.3. P Uptake by Tomato Plants. Tomato plants from both systems, hydroponic and soil-grown, were harvested after 24 days in the growth chamber. Harvested plants were dried in an oven at 65 °C before being combusted at 500 °C for 5 h. Combusted samples were digested with 15 mL of 1 N HCl for 20 min at 220 °C,[43−45] and P was analyzed using IC. The soil pH and the P content in the soil were also examined after 24 days of plant growth experiments, which were carried out in triplicate. The average values of the experimental results are presented.

3. RESULTS AND DISCUSSION

3.1. Characterization. Figure 1(a1−c1) shows X-ray diffractograms for NO_3^--loaded Zn/Al, Mg/Al, and Mg-Zn/Al-LDH. The XRD pattern exhibits well-defined peaks with high crystallinity without any impurity peaks, proving the development of LDHs with a hexagonal layered structure for the NO_3^--loaded LDHs. The basal spacings (d) as calculated by Bragg's law ($n\lambda = 2d \sin\theta$), using the (003) reflection, were 8.9, 8.89, and 8.89 Å for Zn/Al, Mg/Al, and Mg-Zn/Al-LDH, respectively. Berber et al.[46] and Benício et al.[47] reported a d spacing of 8.9 Å for NO_3^--intercalated Mg/Al-LDH. Similar d spacings of 8.84 and 8.53 Å were reported for NO_3^--intercalated Zn/Al-LDH by Mahjoubi et al.[48] and Velu et al.,[49] where the synthesis was done by a coprecipitation method using NaOH in the presence of excess NO_3^- anions; this result has good similarity to the values obtained in this study. The position of the (003) peak and d values are related to the layer charge density, which is the ratio of M^{2+} to M^{3+} ions, the water content of the LDHs, and the arrangement of anions in the interlayer region at various angles relative to the hydroxide sheets.[50,51] The sharpness of the XRD signals for the Zn/Al-LDH showed that LDH was more crystalline than Mg/Al-LDH and Mg-Zn/Al-LDH, as the latter showed broader peaks. The peak broadening could also be attributed to a structural disorder such as stacking faults, higher water content, or Scherrer's broadening due to smaller crystallites leading to a

https://doi.org/10.1021/acsomega.2c07862
ACS Omega 2023, 8, 15017−15030

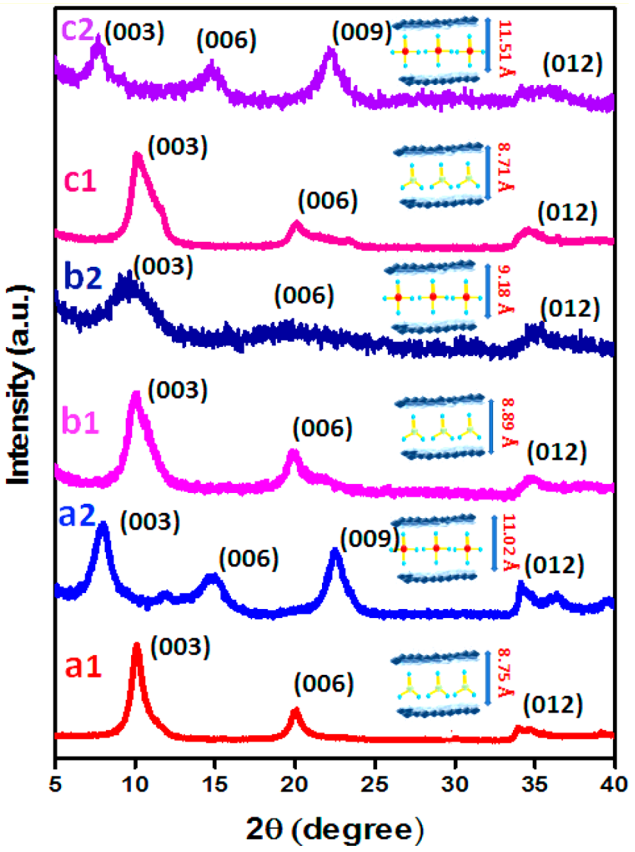

Figure 1. X-ray diffraction peak of the synthesized (a1) N-Zn/Al-LDH, (b1) N-Mg/Al-LDH, and (c1) N-Mg-Zn/Al-LDH and (a2) P-Zn/Al-LDH, (b2) P-Mg/Al-LDH, and (c2) P-Mg-Zn/Al-LDH.

decrease in crystallinity.[49,52] A small asymmetry observed in the 003 peaks of Mg/Al-LDH and Mg-Zn/Al-LDH (Figure 1(b1, c1)) could also indicate the coexistence of the carbonate anion in the interlayer.[53]

Figure 1(a2−c2) shows X-ray diffractograms for P-loaded Zn/Al-LDH, Mg/Al-LDH, and Mg-Zn/Al-LDH after the ion exchange process. P-LDHs showed considerable changes in the diffractograms compared to N-LDHs. The basal spacing increased to 11.02, 9.18, and 11.51 Å for the Zn/Al, Mg/Al, and Mg-Zn/Al-LDH, respectively. Although the increase in the basal spacing indicated an effective exchange of P anions with NO_3^- ions, the different *d* values obtained showed the possibility of different special orientations of P anions in the interlayer of different LDH materials. The XRD patterns of P-LDHs showed fewer crystalline peaks, which could be due to the changes in the layer-by-layer ordering of the LDH lattice along the *c* axis after the ion exchange with P anions in general.[27] However, P-Mg/Al-LDH showed relatively higher peak broadening followed by P-Mg-Zn/Al-LDH, whereas P-Zn/Al-LDH had slightly higher crystallinity, which could be directly correlated to the crystallinity order observed in the N-LDHs.

Frost et al.[54] observed a basal spacing of around 11.9 Å for P-intercalated Zn/Al-LDH, whereas Benicio et al.[55] and Sokol et al.[56] observed basal spacings of 9.12 and 9.9 Å, respectively, for P-intercalated Mg/Al-LDH, which are similar to our observations for P-Zn/Al-LDH and P-Mg/Al-LDH. However, Bernardo et al.[57] observed a basal spacing of around 7.8 Å for P-intercalated Mg/Al-LDH. Furthermore, 8.3 Å basal spacing for P-intercalated Mg/Al-LDH was observed by Everaert et al.[14] The dissimilarity of the peak position and *d* spacing from the reported works could be due to variations in the extent of intercalation of P ions according to changes in the synthesis conditions.

Figure 2(a) displays the XRD pattern of SA with one characteristic peak at 14.28°, which shows an amorphous

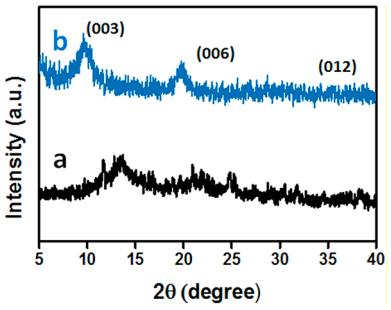

Figure 2. X-ray diffraction peaks of (a) SA and (b) LB.

nature similar to that characterized previously.[58,59] Figure 2(b) shows the XRD diffractogram of LB. The *d* value (003) of 9.23 Å is associated with the value noticed for the P-loaded Mg/Al-LDH, indicating the successful encapsulation of structurally intact P-Mg/Al LDH in the biopolymer matrix.

To better understand the chemical structure and confirm the presence of loaded NO_3^- and P ions, N-LDH and P-LDH materials were characterized by FTIR spectrometry. FTIR spectra of NO_3^--intercalated LDHs are shown in Figure 3(a1−c1). The broad band at 3400 cm^{-1} was attributed to the stretching vibration of hydroxide groups on the surface and interlayer water. The corresponding bending mode of

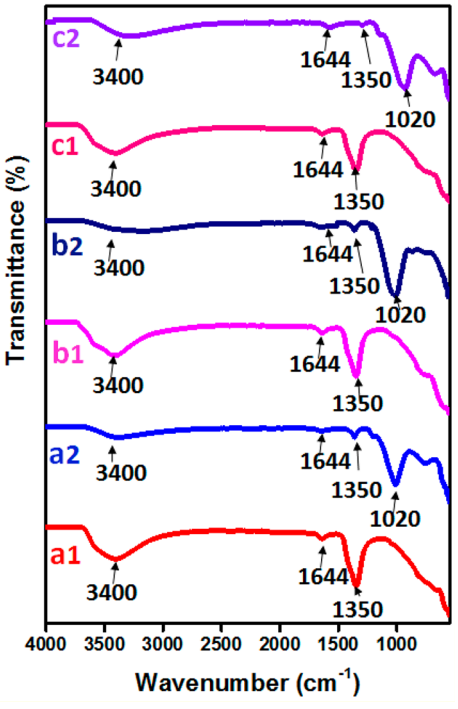

Figure 3. FTIR spectra of the synthesized (a1) N-Zn/Al-LDH, (b1) N-Mg/Al-LDH, and (c1) N Mg-Zn/Al-LDH and (a2) P-Zn/Al-LDH, (b2) P-Mg/Al-LDH, and (c2) P-Mg-Zn/Al-LDH.

https://doi.org/10.1021/acsomega.2c07862
ACS Omega 2023, 8, 15017−15030

interlayer water molecules was observed at 1644 cm^{-1}, while the band at 1350 cm^{-1} was attributed to the vibration modes (ν_3) of NO_3^-, which indicated the effective intercalation of NO_3^- in the interlayer space. The bands at 820 and 667 cm^{-1} were attributed to the vibrational modes (ν_2, ν_4) of NO_3^-.[60,61]

Figure 3(a2−c2) displays the FTIR spectra of P-intercalated LDHs. The spectra of Zn/Al, Mg/Al, and Mg-Zn/Al-LDH are similar. A broad band as in the case of N-LDHs was observed in the 3400 cm^{-1} regions due to the presence of hydroxide groups. The bands at 1020 and 720 cm^{-1} attributed to the stretching vibrational mode (ν_3 and ν_2) of P established the existence of P in the LDHs, which could be attributed to the presence of intercalated $H_2PO_4^-$ species in the LDH layers. Everaert et al.[51] reported pH-dependent speciation in P-intercalated Mg/Al-LDH. The authors reported the presence of HPO_4^{2-}/PO_4^{3-} in LDH synthesized at pH 12, whereas in LDH synthesized at pH 10, HPO_4^{2-} anions were prevalent.

Similar results were obtained by Bencio et al.[47,55] for P-intercalated Mg/Als, Mg/Fe, and Mg/Al/Fe-LDHs. A small band at 1350 cm^{-1} was observed in all of the LDHs, which can be ascribed to the vibrational mode of NO_3^-,[36,55] which could be due to the presence of residual NO_3^- which were not replaced by the P anions during the ion-exchange process. The band at 1350 cm^{-1} is more intense in the case of P-Mg/Al-LDH, indicating a higher retention of NO_3^- ions when compared to Zn/Al and Mg-Zn/Al counterparts. This observation also agrees with the XRD results, where the increase in d spacing obtained was less for P-Mg/Al-LDH as opposed to those of P-Zn/Al-LDH and P-Mg-Zn/Al-LDH.

However, in the FTIR spectra of SA (Figure 4a), the broad band at 3300 cm^{-1} was attributed to the stretching vibration of hydroxide groups. The bands at 1600 and 1412 cm^{-1} were accredited to a stretching vibration (symmetric and asymmetric) of carboxylate groups, whereas the band at 1036 cm^{-1} was indicative of the presence of an ether group.[62] The FTIR spectrum of LB (Figure 4b) reveals that the incorporation of P-Mg/Al-LDH in SA, through the bands at 1620, 1423, and 1327 cm^{-1}, was due to characteristics SA functional groups, while the bands at 1020 and 740 cm^{-1} were associated with the vibrational modes of loaded P-Mg/Al-LDH.

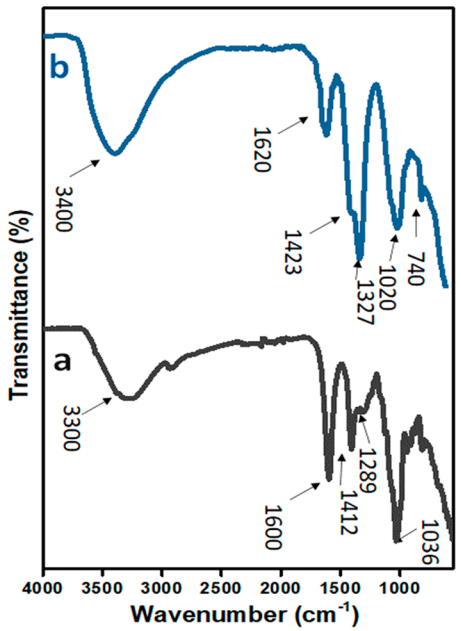

Figure 4. FTIR spectra of (a) SA and (b) LB.

The results of the ICP-OES analysis for the metal element composition and IC analysis for anions of various P-intercalated LDHs are presented in Table 3.

The fractional substitution of Al ions (x value) obtained in LDHs ranged from 0.23 to 0.33, which indicated the proper formation of LDHs with thermodynamic stability. At the synthesis pH of 7, although both $H_2PO_4^-$ and HPO_4^{2-} anions are present in the solution, $H_2PO_4^-$ (pK_a = 7.2) predominates.[63] Based on the stoichiometric ratio, the chemical composition of various LDHs could be represented as $[Zn^{2+}_{0.77072}Al^{3+}_{0.22927}(OH)_2]^{0.22927+}(H_2PO_4^-)_{0.22927-a}(NO_3^-)_a \cdot 0.5(H_2O)$, $[Mg^{2+}_{0.67028}Al^{3+}_{0.32971}(OH)_2]^{0.32971+}(H_2PO_4^-)_{0.32971-b}(NO_3^-)_b \cdot 0.5(H_2O)$, and $[Mg^{2+}_{0.23868}Zn^{2+}_{0.52271}Al^{3+}_{0.23860}(OH)_2]^{0.23860+}(H_2PO_4^-)_{0.23860-c}(NO_3^-)_c \cdot 0.5(H_2O)$, where a, b, and c denoted the residual nitrate present in P-intercalated Zn/Al-LDH, Mg/Al-LDH, and Mg-Zn/Al-LDH, respectively.

TGA analyses were utilized to examine the thermal degradation profiles of P-intercalated Zn/Al-LDH, Mg/Al-LDH, and Mg-Zn/Al-LDH shown in Figure 5(a−c). The TGA/DTG curves for Zn/Al-LDH showed the first mass loss at 40 °C, which was related to physically adsorbed water from the surface, corresponding to 1.65% mass loss.[37,56] The second mass loss at 164 °C (mass loss of 11%) was related to the removal of interlayer water linked to P ions by strong hydrogen bonds.[55,64,65] The third step of mass loss at 236 °C (mass loss of 6%) corresponded to the loss of water molecules through layer dehydroxylation.[57,66] The final mass loss at 534 °C (mass loss of 2%) could be from the decomposition of P ions.[67] For Mg/Al-LDH and Mg-Zn/Al-LDH, the DTG peak positions were at 56 °C (mass loss of 5%), 117 °C (mass loss of 4%), 185 °C (mass loss of 8%), and 411−536 °C (mass loss of 6%) and at 72 °C (mass loss of 4%), 184 °C (mass loss of 5%), 231 °C (mass loss of 5%), and 427 °C (mass loss of 17%), respectively, for surface water, interlayer water, hydroxide groups, and intercalated anion removal or the transition of P ions into metaphosphates.[68] A small peak seen at 304 °C for Mg-Zn/Al-LDH could be due to the transformation of the double layer into a MgO lattice.

Eshaq et al.[69] also found a similar peak position at 300−500 °C for Mg-Zn/Al-LDH; they also obtained the XRD pattern of Mg-Zn/Al LDH after calcination at 450 °C, and the result shows that the LDH phase disappeared and was replaced by the MgO phase. Bernardo et al.[66] found similar mass loss events related to the adsorbed P anions for P-intercalated Ca/Al-LDH. According to the author, increasing the P

Table 3. Chemical Elemental Data of LDH Samples

LDH sample	Zn (mg/g)	Mg (mg/g)	Al (mg/g)	M^{2+}/M^{3+}	P (mg/kg)
P-Zn/Al-LDH	321.7		95.7	3.36	37.8
P-Mg/Al-LDH		197.8	97.3	2.03	42.64
P-Mg-Zn/Al-LDH	221	101.3	101	3.19	44.95

https://doi.org/10.1021/acsomega.2c07862
ACS Omega 2023, 8, 15017−15030

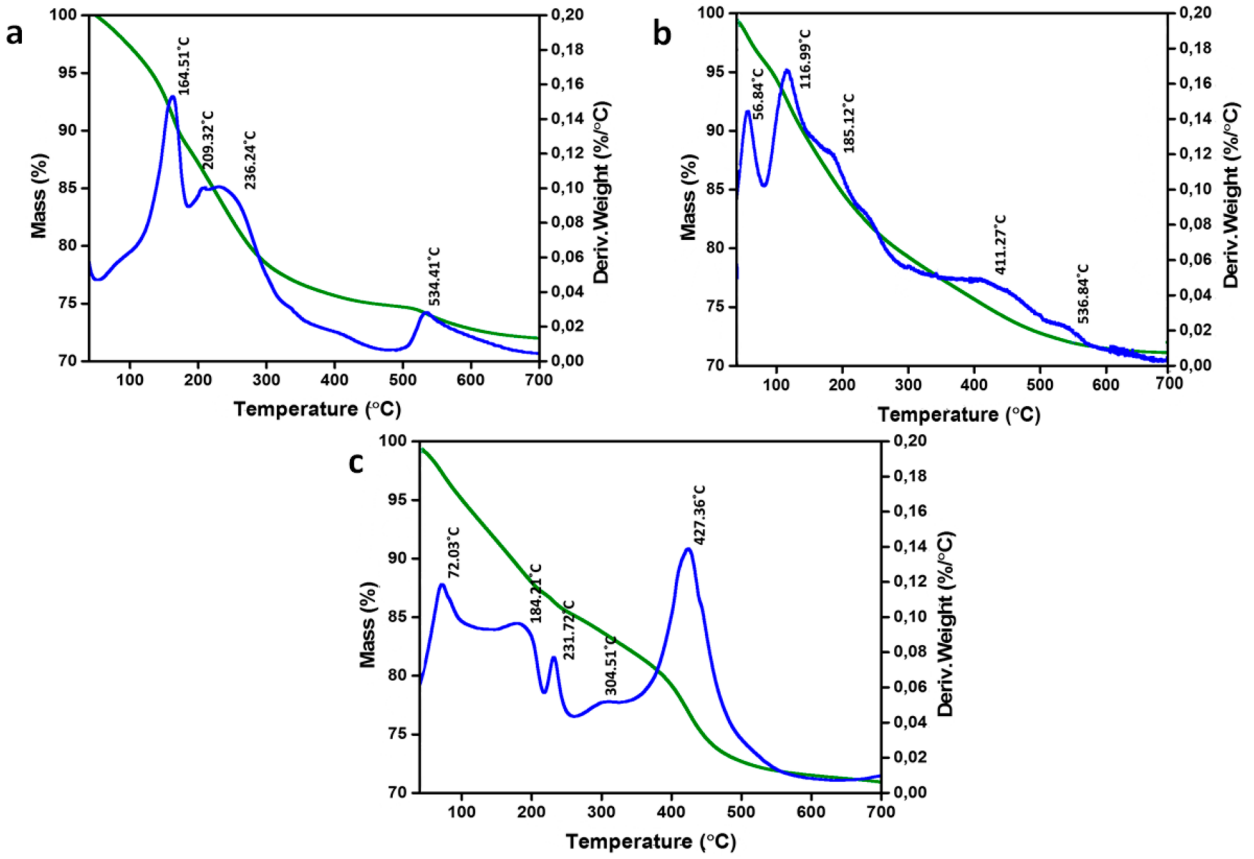

Figure 5. TGA curves of the synthesized (a) P-Zn/Al-LDH, (b) P-Mg/Al-LDH, and (c) P-Mg-Zn/Al-LDH. Green curves show the mass loss percentage, and blue curves show the derivative mass loss.

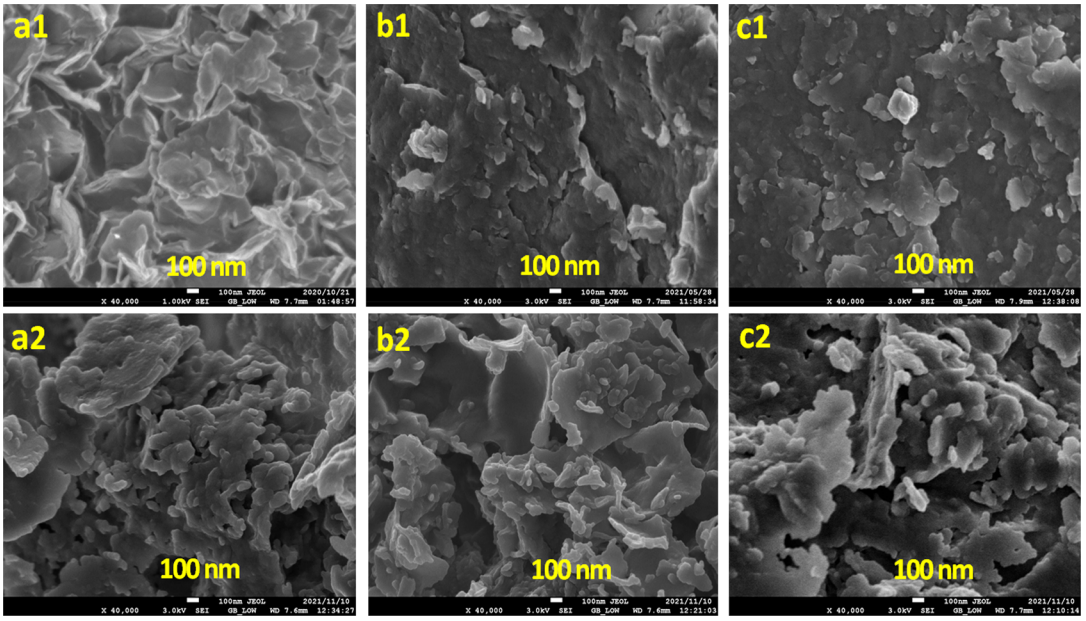

Figure 6. SEM images of the synthesized (a1) N-Zn/Al-LDH, (b1) N-Mg/Al-LDH, and (c1) N Mg-Zn/Al-LDH and (a2) P-Zn/Al-LDH, (b2) P-Mg/Al-LDH, and (c2) P-Mg-Zn/Al-LDH.

concentration for Ca/Al-LDH can decrease mass losses. In another work, Bernardo et al.[37] prepared P-intercalated Zn/Al-LDH using different concentrations of P anions from 0.83 to 33.10 mM. They monitored the decomposition mechanism and concluded that no significant mass loss was observed for 0.83 mm of P, but the losses of adsorbed water and P were found at 208 and 535 °C, respectively, for LDH prepared with 33.10 mM P. However, the decomposition mechanism for LDH synthesized with 16.55 mM P was similar to our observation of P-intercalated Zn/Al-LDH.

https://doi.org/10.1021/acsomega.2c07862
ACS Omega 2023, 8, 15017−15030

SEM images of the NO_3^--intercalated Zn/Al, Mg/Al, and Mg-Zn/Al-LDH are shown in Figure 6(a1−c1). All LDHs exhibited plate-like morphology.[70,71] Zn/Al-LDH displays irregular lamellar structures composed of clearly distinguishable flake-like platelets. On the other hand, Mg/Al-LDH and Mg-Zn/Al-LDH exhibit plate-like platelets but smaller aggregates which were apparent from the XRD peak broadening observed

After P intercalation, significant changes in the LDH structure were seen (Figure 6(a2−c2)). Figure 6(a2, c2) indicated the formation of irregular plates.[64] In contrast, Figure 6(b2) displayed the aggregated flakes with a similar open architecture, including a tiny secondary phase, possibly attributable to adsorbed P.[57,72] Bernardo et al.[66] also observed an irregular morphology of P-intercalated Ca/Al-LDH prepared by the ion-exchange method.

The composite beads LB, on the other hand, exhibited a porous nature with many holes on the surface (Figure 7(a)).

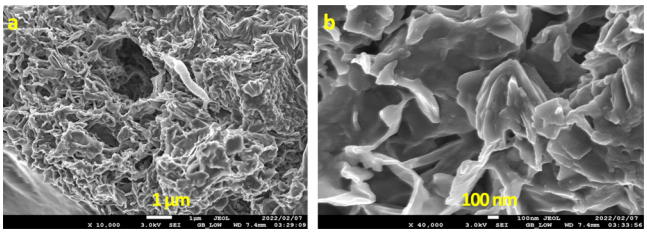

Figure 7. SEM images of LB at different magnifications: (a) 10× and (b) 40×.

Figure 7(b) at higher magnification showed a flake-like structure coated with a polymer, demonstrating that Mg/Al-LDH was successfully encapsulated within the SA matrix. This was confirmed by EDS spectra (Figure 8). Spectra highlighted the existence of Mg and Al cations on the LDH, together with carbon, nitrogen, oxygen, and calcium, as essential elements present in the LB.[73,74]

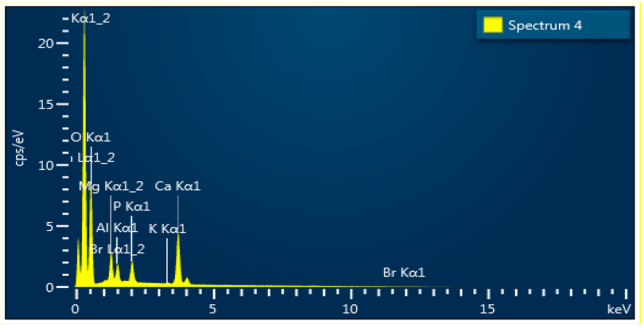

Figure 8. EDS spectra of LB.

3.2. P Release in the Soil Solution. The P release was examined to get an idea of the release properties of various P sources in soil solution, and the release profiles are presented in Figure 9. Approximately 97% of P was released from KH_2PO_4 and Nutrifeed within 0.16 h, predictably for the soluble P source. On the other hand, PS released 56% of P during the first hour and demonstrated the sustained nature of realizing P. The P release from various LDHs follows two steps. Fast release occurs for up to 1 h, associated with the P ions (probably $H_2PO_4^-$ because the charge is less than that of

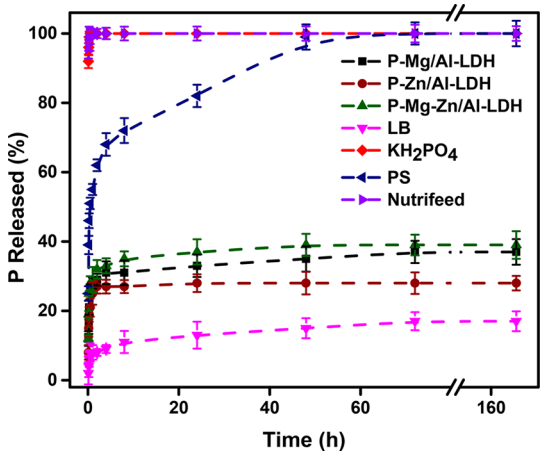

Figure 9. P release from various P sources in the soil solution.

HPO_4^{2-}) on the surface of LDH, usually through electrostatic interactions (weak bonding). The release becomes slow afterward because of the intercalated HPO_4^{2-} ion (with the higher charge), which is exchanged slowly with the existing OH^- and CO_2^{3-} ions in the medium.[55,75]

The results of the P release in the soil solution demonstrated that after 60 min the LDHs started to release P gradually. The release rates after 1 h were 28, 24, and 29% for P-Mg/Al, P-Zn/Al, and P-Mg-Zn/Al-LDH; the release rates after 168 h were 37, 27, and 39%. Moreover, the P releases from P-Mg/Al and P-Mg-Zn/Al-LDH were similar, but the P-Zn/Al-LDH showed a slower release rate than the other two LDHs, probably because of the structural organization. Silva et al.[76] proposed that intercalation provided the physical protection of anions that helped to release intercalated anions slowly. The crystallinity of the material as well as the interlayer ionic barrier also played a vital role in the slow release, which is in agreement with the release profiles obtained in this work. P-Zn/Al-LDH showed relatively higher crystallinity according to the XRD patterns, and this sample showed the slowest release of P ions out of the three P-LDHs. Besides crystallinity, considering the solubility product constants (K_{sp}) of zinc, magnesium, aluminum, and hydroxides at 25 °C in a basic medium, which are 3×10^{-17}, 5.6×10^{-12}, 1.9×10^{-33}, and 3×10^{-34}, respectively, it was suggested that the Zn-bearing LDH phases were more structurally stable and less soluble than the Mg-containing LDHs, which could also be a reason for the slow release of P ions from Zn/Al-LDH.[77] As reported by Bernardo et al.[56] during the first 53 min, the release of P was 90% by using a bicarbonate solution (3.33×10^{-3} M). However, 50% of the P release was observed by Everaert et al.[14] during 1000 h on the release medium containing 2.2 mM bicarbonate solution. However, Benicio et al.[55] noticed that 60% of the P was released after 150 min while using deionized water. According to the author, the release happened due to the interaction of P-Mg/Al-LDH with the carbonate ion present in water. Our P release rates in the soil solution were higher compared to those of Onishi et al.;[78] they obtained 11 and 5.5% P released from P-modified Mg/Al-LDH in clayey and sandy soil solutions after 1080 h. The existence of various anions in the soil solution that results in a competitive exchange process with anions in LDH was suggested as the reason for the slow release rate.

A pH-buffering property was also observed for all of the P-LDHs in the soil solution. After 168 h of the release of P, the

https://doi.org/10.1021/acsomega.2c07862
ACS Omega 2023, 8, 15017−15030

pH of the soil solution was significantly changed from an initial value of 6.5 to 7.25, 8.44, and 7.92 for P-Zn/Al, P-Mg/Al, and P-Mg-Zn/Al-LDH, respectively. In these pH values, both $H_2PO_4^-$ and HPO_4^{2-} probably exists. Because of the higher pH, the primary existence of P species was HPO_4^{2-} for Mg/Al-LDH. Contrary to this observation, the soil solution pH decreased to 5.2 for PS, and nutrified solution showed the lowest pH of 4.5. In these pH values, only $H_2PO_4^-$ exists, meaning that P-LDHs could supply mono- and divalent P species to the medium. P-Zn/Al-LDH showed the lowest buffering capacity, while P-Mg/Al-LDH offered the highest buffering capacity. Sieda et al.[79] employed carbonate forms of Ca/Fe-LDH and Mg/Fe-LDH for P removal from aqueous solutions and suggested that the buffering pH effect of LDH was due to the release of metal cations (Mg^{2+}, Ca^{2+}, and Fe^{3+}) and/or their hydroxides. The facts could justify the higher buffering capacity of P-Mg/Al-LDH in that Mg^{2+} forms stronger ionic bonds with hydroxide groups[80] and magnesium hydroxide has the highest solubility constant, leading to easy solubilization and a faster release of hydroxide ions in the aqueous medium in comparison to the LDHs containing Zn.[77] The anions captured in the interlayer of the LDHs could also affect the pH buffer action of the LDHs. According to Shibata et al.,[80] slurried LDHs showed equilibrium pH due to buffering action, where LDHs intercalated with divalent anions showed higher pH than those with monovalent anions. During the process, H^+ from the aqueous medium could be consumed by interlayer ions, such as CO_3^{2-}, HPO_4^{2-}, or $H_2PO_4^-$. Hence, the higher buffering capacity observed in the case of P-Mg/Al-LDH could also be due to the presence of CO_3^{2-} in the interlayer.

Mg/Al-LDH was chosen to prepare the LB due to its better buffering and suitable P-release ability. The release rate of P from LB was lower than that of P-LDHs; these results were expected since the surface area of alginate is much lower than that of the powdered form of LDHs. LB released P only 16% after 168 h, and the pH of the soil solution increased to 7.04. The slowest release of P observed from LB can be attributed to encapsulation in the biopolymer matrix, providing an additional barrier to the diffusion of P ions. However, LB showed moderate buffering capacity as the buffering capacity of the alginate beads depends on the coordinate binding by carboxylate groups and the dehydration ratio of alginate beads as well as the solution pH.[81,82]

3.3. P Release by LDHs in a Hydroponic System. A hydroponic system was suggested as a more economical procedure for using inorganic nutrients to grow tomato plants because nutrients can be recycled.[83] The application of a slow-release fertilizer in a hydroponic system can deliver nutrients according to the plant's nutrient requirements. Therefore, the tomato plant was used in a hydroponic system to evaluate the P release properties of prepared LDH with soluble P source KH_2PO_4 and commercial fertilizer Nutrifeed. The results determined that the dry matter production and the P uptake by the plant were higher for Nutrifeed and KH_2PO_4 compared to those of LDHs (Table 4). LB was excluded from this study as the P release was the slowest of all of the prepared materials.

The dry matter was lower for plants treated with LDHs in general when compared to those of Nutrifeed and KH_2PO_4. This was consistent with the release pattern presented in Figure 9. P-Mg-Zn/Al-LDH had the highest release rate of P in the soil solution, which was close to that of P-Mg/Al-LDH.

Table 4. Dry Matter, P Content, and pH Obtained in a Hydroponic System

sample	dry matter of tomato plants (g/bucket)	P content in tomato plant (mg/bucket)	pH of the solutions after the experiment
control	0.35 ± 0.07		6.05 ± 0.04
KH_2PO_4	1.52 ± 0.15	6.71 ± 0.61	6.78 ± 0.03
P-Mg/Al-LDH	1.02 ± 0.11	3.81 ± 0.22	8.21 ± 0.09
P-Zn/Al-LDH	0.68 ± 0.06	1.87 ± 0.21	7.12 ± 0.07
P-Mg-Zn/Al-LDH	0.95 ± 0.08	1.88 ± 0.09	7.98 ± 0.06
Nutrifeed	1.67 ± 0.73	7.66 ± 0.77	4.42 ± 0.21

The dry matter production was the lowest in the control and was the highest in the case of Nutrifeed.

The P uptake by the plant indicated that although LDHs could supply P, the uptake was higher for plants treated with KH_2PO_4 and Nutrifeed, which could be due to the crystalline nature of LDHs and the slow dissolution process. A higher pH value was acquired for the nutrient medium when LDHs were utilized as a fertilizer. The increase in soil pH by the use of LDHs could be due to the anion exchange between the anions present in the soil and the nitrate. The pH of the Nutrifeed solution was much lower, indicating the acidification of the medium by the fertilizer.

When LDHs are applied as fertilizers, intercalated P anions are released slowly by ion exchange with anions present in the medium.[84] Therefore, in the hydroponic system, the root growth of the tomato plants after 17 days from LDHs was significantly lower compared to that from Nutrifeed and KH_2PO_4 because of the immediate availability of P for plants from the soluble sources (Figure 10). On the other hand, no root growth was observed in the control experiment. Of the various LDHs, P-Zn/Al-LDH showed the lowest root growth compared to the other LDHs (P-Mg/Al-LDH and P-Mg-Zn/Al-LDH). This observation is in agreement with the P-release patterns, where P-Zn/Al-LDH had the slowest release rate in the soil solution, which could be due to the relatively higher crystallinity as evident from the XRD results as well as due to

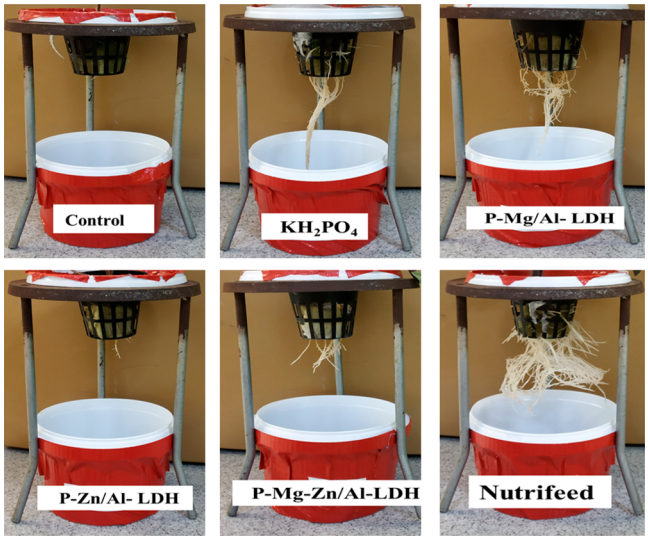

Figure 10. Visual comparison between tomato plant and root growth in a hydroponic system with water-soluble fertilizer and LDHs on day 17. A.S.R., the first author of this article, took digital images.

https://doi.org/10.1021/acsomega.2c07862
ACS Omega 2023, 8, 15017−15030

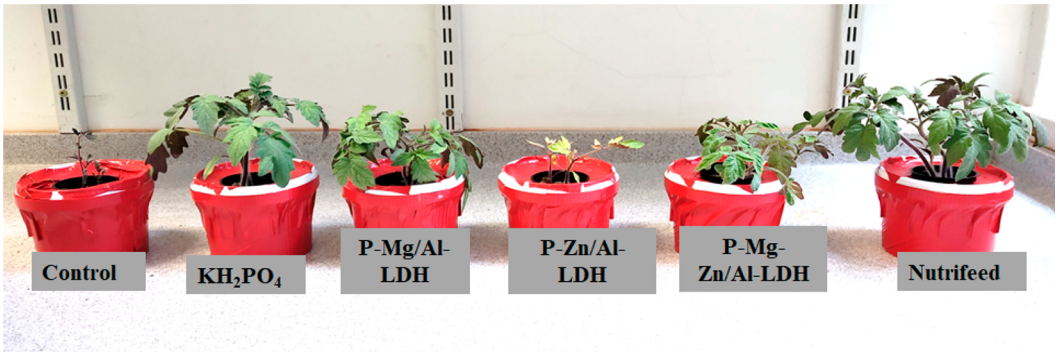

Figure 11. Visual comparison of tomato plants grown in a hydroponic system on day 24 using different fertilizer materials. A.S.R., the first author of this article, took digital images.

Table 5. Dry Matter, P Content, and pH Obtained in a Soil System

sample	dry matter of tomato plants (g/pot)	P content in tomato plant (mg/pot)	pH of the solutions after 24 days	available P (mg/pot)
control	0.71 ± 0.04	2.35 ± 0.25	6.12 ± 0.04	0.67 ± 0.05
KH_2PO_4	1.82 ± 0.11	6.83 ± 0.89	6.37 ± 0.06	3.21 ± 0.15
P-Mg/Al-LDH	1.72 ± 0.16	6.68 ± 0.73	8.38 ± 0.05	6.78 ± 0.79
P-Zn/Al-LDH	1.38 ± 0.07	5.12 ± 0.47	7.11 ± 0.09	7.31 ± 0.81
P-Mg-Zn/Al-LDH	1.67 ± 0.13	6.65 ± 0.81	7.97 ± 0.05	6.87 ± 0.71
LB	0.82 ± 0.03	1.96 ± 0.18	7.01 ± 0.06	3.15 ± 0.11
PS	1.58 ± 0.14	6.48 ± 0.68	5.26 ± 0.18	3.36 ± 0.51

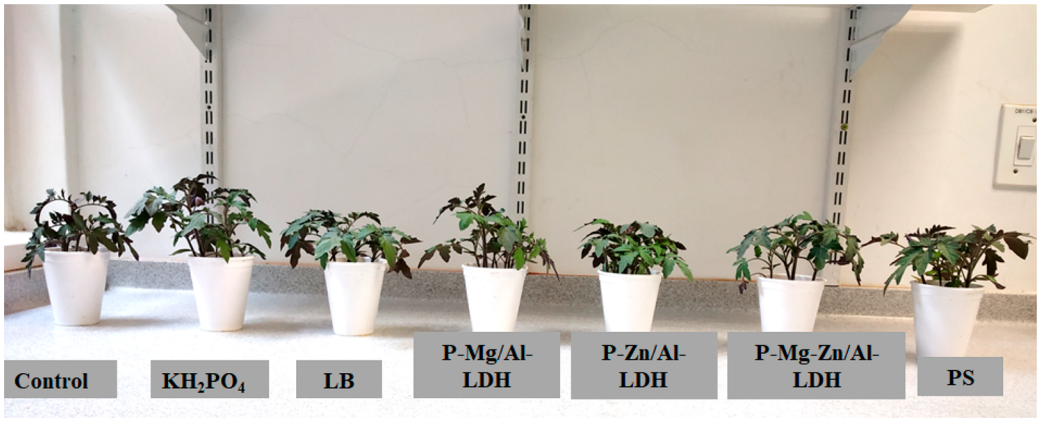

Figure 12. Visual comparison between tomato plants grown in a soil system on day 24 using different fertilizer materials. A.S.R., the first author of this article, took digital images.

the lower solubility of Zn/Al-LDH in comparison to the Mg-bearing LDHs.[77]

After 24 days of sowing, the growth of the plant was lower for LDHs compared to that for soluble P sources (Figure 11). The P release may be enhanced by using a carbonate solution, which was already observed.[14,57] Trientini et al.[85] used controlled-release fertilizer to grow basil in a hydroponic system and found a slower release of P relative to N and K; these results were due to the lower solubility of P ions in contrast with the other ions, mainly NO_3^- and NH_4^+.[86] However, further research in this manner is required for optimum results.

3.4. P Release by LDHs and LB in a Soil System. The soil and P source interaction was essential for dry matter production. The data obtained on the effects of Zn/Al-LDH, Mg/Al-LDH, Mg-Zn/Al-LDH, LB, KH_2PO_4, and PS on soil and plant characteristics are presented in Table 5.

The dry matter production of LDHs (P-Mg/Al-LDH and P-Mg-Zn/Al-LDH) showed 1.6−1.7 g compared to 1.8 g when KH_2PO_4 was used and 1.5 g when PS was used. The P contents in the tomato plants were 6.68, 6.65, 6.83, and 6.48 mg/pot for LDHs (P-Mg/Al-LDH and P-Mg-Zn/Al-LDH), KH_2PO_4, and PS, respectively. From the results, it is evident that Mg-containing LDHs were capable of supplying P to the tomato plants in an equivalent amount as the commercial soluble fertilizer, whereas the slow-release commercial fertilizer was performing slightly inferior to the LDHs P-Zn/Al-LDH and showed less dry matter production and P content than other LDHs, probably due to the more gradual release properties of P-Zn/Al-LDH as described in our soil solution experiments.

The soil pH values after harvest showed higher values when LDHs were used in the powder form. The Mg/Al-LDH showed the highest pH change (8.3) of all of the LDHs. In tropical soils, an increase in the pH also increases the maintenance of P in the soil solution, which increases P availability to plants due to lower anion adsorption.[87,88] The anion adsorption (P) was decreased due to the negatively

https://doi.org/10.1021/acsomega.2c07862
ACS Omega 2023, 8, 15017−15030

charged soil matrix. Devau et al.[89] demonstrated that an increasing soil pH value could release P anions weakly bound to kaolinite and goethite. When the spreading of P in the soil increases, plants can take up the nutrient, which leads to more production.[55] On the other hand, a decrease in soil pH was observed for PS, showing its disadvantage in terms of acidification of the soil. Furthermore, the P availability in the soil was higher for LDHs (Table 5), which means a significant amount of the P was accessible from interaction with the soil and is available to plants for absorption for a more extended period, which can remain usable for the next crop season.

Out of the materials tested, LB showed the lowest efficacy toward dry matter production, P uptake, P availability, and buffering capacity. The decreased surface area of LB as well as the physical barrier offered by the alginate could have prevented the LDH in LB from being exposed to the soil. Moreover, the alginate also forms an electrostatic obstruction that decreases the exchange rate of P with other anions.[24]

Figure 12 shows the growth of tomato plants after 24 days with different fertilizer treatments, along with the control. A comparison of the pictures clearly shows similar plant growth with LDH treatment when compared to the commercial fertilizer PS, although the pot with soluble fertilizer KH_2PO_4 showed slightly better growth of the plant. In the control and LB experiments, weaker plant growth was observed under similar growth conditions. This was consistent with the results documented in Figure 9 and Table 5. This study has shown that P from LDH has excellent potential for direct use as a slow-release P fertilizer under soil conditions.

4. CONCLUSIONS

This study described the synthesis of various P-modified LDHs through the anion exchange method using the corresponding NO_3^--intercalated LDHs. All of the prepared materials showed slow-release properties in the soil solution; the outcome showed a much more gradual release than commercial soluble and slow-release fertilizers. A comparison of the fertilizer efficiency of the P-intercalated LDHs in two different plant growth systems (hydroponic and soil) showed that the LDHs were less effective under hydroponic conditions than under soil conditions. In hydroponic experiments, the soluble P source (KH_2PO_4, Nutrifeed) resulted in better plant growth and dry matter production after 24 days. However, P-Mg/Al-LDH and P-Mg-Zn/Al-LDH showed comparable performance in plant growth, dry matter production, pH buffering, and P availability in soil, demonstrating their excellent prospects as slow-release fertilizers in the soil. However, further study is required to optimize the application methods to take advantage of the full potential of the materials.

■ ASSOCIATED CONTENT

Supporting Information

The Supporting Information is available free of charge at https://pubs.acs.org/doi/10.1021/acsomega.2c07862.

X-ray diffraction pattern of the synthesized P-Zn/Al-LDH in 1 and 0.3 M KH_2PO_4 solution; growth chamber experiment with tomato plants in hydroponic and soil system on day 24 using different fertilizer materials (PDF)

■ AUTHOR INFORMATION

Corresponding Author

Suprakas Sinha Ray − *Department of Chemical Sciences, University of Johannesburg, Doorfontein 2028 Johannesburg, South Africa; Centre for Nanostructures and Advanced Materials, DSI-CSIR Nanotechnology Innovation Centre, Council for Scientific and Industrial Research, Pretoria 0001, South Africa;* orcid.org/0000-0002-0007-2595; Email: rsuprakas@csir.co.za, ssinharay@uj.ac.za

Authors

Abhinandan Singha Roy − *Department of Chemical Sciences, University of Johannesburg, Doorfontein 2028 Johannesburg, South Africa; Centre for Nanostructures and Advanced Materials, DSI-CSIR Nanotechnology Innovation Centre, Council for Scientific and Industrial Research, Pretoria 0001, South Africa;* orcid.org/0000-0002-6464-605X

Marinda de Beer − *Centre for Nanostructures and Advanced Materials, DSI-CSIR Nanotechnology Innovation Centre, Council for Scientific and Industrial Research, Pretoria 0001, South Africa*

Sreejarani Kesavan Pillai − *Centre for Nanostructures and Advanced Materials, DSI-CSIR Nanotechnology Innovation Centre, Council for Scientific and Industrial Research, Pretoria 0001, South Africa;* orcid.org/0000-0001-8015-2941

Complete contact information is available at: https://pubs.acs.org/10.1021/acsomega.2c07862

Notes

The authors declare no competing financial interest.

■ ACKNOWLEDGMENTS

The authors are grateful to the CSIR and the Department of Science and Innovation (C6EEM29), South Africa. A.S.R. thanks the University of Johannesburg for financial support (student no. 219053157).

■ REFERENCES

(1) Schachtman, D. P.; Reid, R. J.; Ayling, S. M. Phosphorus uptake by plants: from soil to cell. *Plant Physiol.* **1998**, *116*, 447−453.

(2) Hinsinger, P. Bioavailability of soil inorganic P in the rhizosphere as affected by root-induced chemical changes: a review. *Plant Soil* **2001**, *237*, 173−195.

(3) Maertens, E.; Thijs, A.; Smolders, E.; Degryse, F.; Cong, P.; Merckx, R. An anion resin membrane technique to overcome detection limits of isotopically exchanged P in P-sorbing soils. *Eur. J. Soil Sci.* **2004**, *55*, 63−69.

(4) Childers, D. L.; Corman, J.; Edwards, M.; Elser, J. J. Sustainability challenges of phosphorus and food: solutions from closing the human phosphorus cycle. *Bioscience* **2011**, *61*, 117−124.

(5) Oliveira, C.; Alves, V.; Marriel, I.; Gomes, E.; Scotti, M.; Carneiro, N.; Guimaraes, C.; Schaffert, R.; Sá, N. Phosphate solubilizing microorganisms isolated from rhizosphere of maize cultivated in an oxisol of the Brazilian Cerrado Biome. *Soil Biol. Biochem.* **2009**, *41*, 1782−1787.

(6) Malhi, S.; Haderlein, L.; Pauly, D.; Johnston, A. Improving fertilizer phosphorus use efficiency. *Development* **2002**, *85*, 18−23.

(7) Weld, J. L.; Parsons, R. L.; Beegle, D. B.; Sharpley, A. N.; Gburek, W. J.; Clouser, W. R. Evaluation of phosphorus-based nutrient management strategies in Pennsylvania. *J. Soil Water Conserv.* **2002**, *57*, 448−454.

(8) Bolan, N.; Hedley, M. Dissolution of phosphate rocks in soils. 1. Evaluation of extraction methods for the measurement of phosphate rock dissolution. *Fertilizer research* **1989**, *19*, 65−75.

(9) Rajan, S. Phosphate rock and phosphate rock/sulphur granules as phosphate fertilizers and their dissolution in soil. *Fertilizer research* **1987**, *11*, 43−60.
(10) Yang, Y.; He, Z.; Yang, X.; Fan, J.; Stoffella, P.; Brittain, C. Dolomite phosphate rock-based slow-release fertilizer for agriculture and landscapes. *Commun. Soil Sci. Plant Anal.* **2012**, *43*, 1344−1362.
(11) Yang, Y.; He, Z.; Yang, X.; Stoffella, P. J. Dolomite phosphate rock (DPR) application in acidic sandy soil in reducing leaching of phosphorus and heavy metals—a column leaching study. *Environ. Sci. Pollut. Res.* **2013**, *20*, 3843−3851.
(12) Ahmad, N.; Fernando, W.; Uzir, M. Parametric evaluation using mechanistic model for release rate of phosphate ions from chitosan-coated phosphorus fertilizer pellets. *Biosyst. Eng.* **2015**, *129*, 78−86.
(13) Pauly, D.; Malhi, S.; Nyborg, M. 2002. Controlled-release P fertilizer concept evaluation using growth and P uptake of barley from three soils in greenhouse. *Can. J. Soil Sci.* **2002**, *82*, 201−210.
(14) Everaert, M.; Warrinnier, R.; Baken, S.; Gustafsson, J.; De Vos, D.; Smolders, E. Phosphate-exchanged Mg-Al layered double hydroxides: a new slow release phosphate fertilizer. *ACS Sustain. Chem. Eng.* **2016**, *4*, 4280−4287.
(15) Liu, R.; Lal, R. Synthetic apatite nanoparticles as a phosphorus fertilizer for soybean (Glycine max). *Sci. Rep.* **2014**, *4*, 5686.
(16) An, X.; Wu, Z.; Liu, X.; Shi, W.; Tian, F.; Yu, B. A new class of biochar-based slow-release phosphorus fertilizers with high water retention based on integrated co-pyrolysis and co-polymerization. *Chemosphere* **2021**, *285*, 131481.
(17) Zhang, S.; Gao, N.; Shen, T.; Yang, Y.; Gao, B.; Li, Y. C.; Wan, Y. One-step synthesis of superhydrophobic and multifunctional nano copper-modified bio-polyurethane for controlled-release fertilizers with "multilayer air shields": new insight of improvement mechanism. *J. Mater. Chem. A* **2019**, *7*, 9503−9509.
(18) Zhang, S.; Shen, T.; Yang, Y.; Li, Y. C.; Wan, Y.; Zhang, M.; Tang, Y.; Allen, S. C. Controlled-release urea reduced nitrogen leaching and improved nitrogen use efficiency and yield of direct-seeded rice. *J. Environ. Manage.* **2018**, *220*, 191−197.
(19) Konta, J. Clay and man: clay raw materials in the service of man. *Appl. Clay Sci.* **1995**, *10*, 275−335.
(20) Roy, A. S.; Pillai, S. K.; Ray, S. S. Layered Double Hydroxides for Sustainable Agriculture and Environment: An Overview. *ACS Omega.* **2022**, *7*, 20428.
(21) Buates, J.; Imai, T. Assessment of plant growth performance and nutrient release for application of phosphorus-loaded layered double hydroxides as fertilizer. *Environ. Technol. Innov.* **2021**, *22*, 101505.
(22) López-Rayo, S.; Imran, A.; Bruun Hansen, H. C.; Schjoerring, J. K.; Magid, J. Layered double hydroxides: potential release-on-demand fertilizers for plant zinc nutrition. *J. Agric. Food Chem.* **2017**, *65*, 8779−8789.
(23) Everaert, M.; Smolders, E.; McLaughlin, M. J.; Andelkovic, I.; Smolders, S.; Degryse, F. Layered Double Hydroxides as Slow-Release Fertilizer Compounds for the Micronutrient Molybdenum. *J. Agric. Food Chem.* **2021**, *69*, 14501−14511.
(24) Everaert, M.; Degryse, F.; McLaughlin, M. J.; De Vos, D.; Smolders, E. Agronomic effectiveness of granulated and powdered P-exchanged Mg-Al LDH relative to struvite and MAP. *J. Agric. Food Chem.* **2017**, *65*, 6736−6744.
(25) Witzke, T.; Torres-Dorante, L.; Bullerjahn, F.; Pöllmann, H. Use of layered double hydroxides (LDH) of the hydrotalcite group as reservoir minerals for nitrate in soils-examination of the chemical and mechanical stability. In *Minerals as Advanced Materials II*; Springer: Berlin, 2011; pp 131−145.
(26) Parello, M. L.; Rojas, R.; Giacomelli, C. E. Dissolution kinetics and mechanism of Mg-Al layered double hydroxides: a simple approach to describe drug release in acid media. *J. Colloid Interface Sci.* **2010**, *351*, 134−139.
(27) Woo, M. A.; Kim, T. W.; Paek, M.; Ha, H.; Choy, J.; Hwang, S. Phosphate-intercalated Ca-Fe-layered double hydroxides: Crystal structure, bonding character, and release kinetics of phosphate. *J. Solid State Chem.* **2011**, *184*, 171−176.
(28) Chitrakar, R.; Tezuka, S.; Sonoda, A.; Sakane, K.; Ooi, K.; Hirotsu, T. Adsorption of phosphate from seawater on calcined MgMn-layered double hydroxides. *J. Colloid Interface Sci.* **2005**, *290*, 45−51.
(29) Khaldi, M.; Badreddine, M.; Legrouri, A.; Chaouch, M.; Barroug, A.; De Roy, A.; Besse, J. Preparation of a well-ordered layered nanocomposite from zinc-aluminum-chloride layered double hydroxide and hydrogenophosphate by ion exchange. *Mater. Res. Bull.* **1998**, *33*, 1835−1843.
(30) Costantino, U.; Casciola, M.; Massinelli, L.; Nocchetti, M.; Vivani, R. Intercalation and grafting of hydrogen phosphates and phosphonates into synthetic hydrotalcites and ac-conductivity of the compounds thereby obtained. *Solid State Ion.* **1997**, *97*, 203−212.
(31) Koilraj, P.; Antonyraj, C. A.; Gupta, V.; Reddy, C.; Kannan, S. Novel approach for selective phosphate removal using colloidal layered double hydroxide nanosheets and use of residue as fertilizer. *Appl. Clay Sci.* **2013**, *86*, 111−118.
(32) Halajnia, A.; Oustan, S.; Najafi, N.; Khataee, A.; Lakzian, A. Effects of Mg-Al layered double hydroxide on nitrate leaching and nitrogen uptake by maize in a calcareous soil. *Commun. Soil Sci. Plant Anal.* **2016**, *47*, 1162−1175.
(33) de Castro, G. F.; Ferreira, J. A.; Eulálio, D.; de Souza, S. J.; Novais, S. V.; Novais, R. F.; Pinto, F. G.; Tronto, J. Layered double hydroxides: matrices for storage and source of boron for plant growth. *Clay Miner.* **2018**, *53*, 79−89.
(34) Wang, B.; Gao, B.; Zimmerman, A. R.; Zheng, Y.; Lyu, H. Novel biochar-impregnated calcium alginate beads with improved water holding and nutrient retention properties. *J. Environ. Manage.* **2018**, *209*, 105−111.
(35) Bokkhim, H.; Bansal, N.; Grøndahl, L.; Bhandari, B. Characterization of alginate-lactoferrin beads prepared by extrusion gelation method. *Food Hydrocoll.* **2016**, *53*, 270−276.
(36) Badreddine, M.; Legrouri, A.; Barroug, A.; De Roy, A.; Besse, J. Ion exchange of different phosphate ions into the zinc-aluminium-chloride layered double hydroxide. *Mater. Lett.* **1999**, *38*, 391−395.
(37) Bernardo, M. P.; Ribeiro, C. Zn-Al-based layered double hydroxides (LDH) active structures for dental restorative materials. *J. Mater. Res. Technol.* **2019**, *8*, 1250−1257.
(38) Bouyoucos, G. J. Hydrometer method improved for making particle size analyses of soils 1. *Agron J.* **1962**, *54*, 464−465.
(39) Okalebo, J. R.; Gathua, K. W.; Woomer, P. L. *Laboratory Methods of Soil and Plant Analysis: A Working Manual*, 2nd ed.; Sacred Africa, Nairobi Office, 2002; Vol. *21*, pp 25, 26.
(40) Pleysier, J. L.; Juo, A. S. R. A single-extraction method using silver-thiourea for measuring exchangeable cations and effective CEC in soils with variable charges. *Soil Sci.* **1980**, *129*, 205−211.
(41) Turrión, M. B.; Gallardo, J. F.; González, M. I. Extraction of soil-available phosphate, nitrate, and sulphate ions using ion exchange membranes and determination by ion exchange chromatography. *Commun. Soil Sci. Plant Anal.* **1999**, *30*, 1137−1152.
(42) Schulte, E. E.; Hoskins, B. Recommended Soil Organic Matter Tests. Recommended Soil Testing Procedures for the Northeastern United States. *Northeastern Regional Publication*; University of Delaware: 1995; Vol. *493*, pp 52−60.
(43) Berthold, M.; Zimmer, D.; Schumann, R. A simplified method for total phosphorus digestion with potassium persulphate at sub-boiling temperatures in different environmental samples. *Rostock. Meeresbiol. Beitr.* **2015**, *25*, 7−25.
(44) Habibzadeh, Y. Effects of phosphorus levels on dry matter production and root traits of chickpea plants in presence or absence of Arbuscular mycorrhizal fungi. *J. Agric. Sci. Food Sci. Technol.* **2015**, *1*, 1−6.
(45) Andersen, J. M. An ignition method for determination of total phosphorus in lake sediments. *Water Res.* **1976**, *10*, 329−331.
(46) Berber, M. R.; Hafez, I. H. Synthesis of a new nitrate-fertilizer form with a controlled release behavior via an incorporation technique into a clay material. *Bull. Environ. Contam. Toxicol.* **2018**, *101*, 751−757.

https://doi.org/10.1021/acsomega.2c07862
ACS Omega 2023, 8, 15017−15030

(47) Benício, L. P. F.; Eulálio, D.; Guimarães, L. D. M.; Pinto, F. G.; Costa, L. M. D.; Tronto, J. Layered double hydroxides as hosting matrices for storage and slow release of phosphate analyzed by stirred-flow method. *Mater. Res.* **2018**, *21*, No. e20171004.
(48) Mahjoubi, F. Z.; Khalidi, A.; Abdennouri, M.; Barka, N. Zn-Al layered double hydroxides intercalated with carbonate, nitrate, chloride and sulphate ions: Synthesis, characterization and dye removal properties. *J. Taibah Univ. Sci.* **2017**, *11*, 90−100.
(49) Velu, S.; Ramkumar, V.; Narayanan, A.; Swamy, C. Effect of interlayer anions on the physicochemical properties of zinc-aluminium hydrotalcite-like compounds. *J. Mater. Sci.* **1997**, *32*, 957−964.
(50) Zhitova, E. S.; Krivovichev, S. V.; Pekov, I. V.; Yakovenchuk, V. N.; Pakhomovsky, Y. A. Correlation between the d-value and the M2+: M3+ cation ratio in Mg-Al-CO3 layered double hydroxides. *Appl. Clay Sci.* **2016**, *130*, 2−11.
(51) Everaert, M.; Dox, K.; Steele, J. A.; De Vos, D.; Smolders, E. Solid-state speciation of interlayer anions in layered double hydroxides. *J. Colloid Interface Sci.* **2019**, *537*, 151−162.
(52) Ellis, J. E.; Kim, K. J.; Cvetic, P. C.; Ohodnicki, P. R. In Situ Growth and Interlayer Modulation of Layered Double Hydroxide Thin Films from a Transparent Conducting Oxide Precursor. *Cryst. Growth Des.* **2021**, *21*, 1518−1526.
(53) Conterosito, E.; Palin, L.; Antonioli, D.; Viterbo, D.; Mugnaioli, E.; Kolb, U.; Perioli, L.; Milanesio, M.; Gianotti, V. Structural Characterisation of Complex Layered Double Hydroxides and TGA-GC-MS Study on Thermal Response and Carbonate Contamination in Nitrate-and Organic-Exchanged Hydrotalcites. *Chem.—Eur. J.* **2015**, *21*, 14975−14986.
(54) Frost, R. L.; Musumeci, A. W.; Kloprogge, J. T.; Adebajo, M. O.; Martens, W. N. Raman spectroscopy of hydrotalcites with phosphate in the interlayer: implications for the removal of phosphate from water. *J. Raman Spectrosc.* **2006**, *37*, 733−741.
(55) Benício, L. P. F.; Constantino, V. R. L.; Pinto, F. G.; Vergütz, L.; Tronto, J.; da Costa, L. M. Layered double hydroxides: new technology in phosphate fertilizers based on nanostructured materials. *ACS Sustain. Chem. Eng.* **2017**, *5*, 399−409.
(56) Sokol, D.; Vieira, D. E.; Zarkov, A.; Ferreira, M. G.; Beganskiene, A.; Rubanik, V. V.; Shilin, A. D.; Kareiva, A.; Salak, A. N. Sonication accelerated formation of Mg-Al-phosphate layered double hydroxide via sol-gel prepared mixed metal oxides. *Sci. Rep.* **2019**, *9*, 10419.
(57) Bernardo, M. P.; Guimaraes, G. G.; Majaron, V. F.; Ribeiro, C. Controlled release of phosphate from layered double hydroxide structures: dynamics in soil and application as smart fertilizer. *ACS Sustain. Chem. Eng.* **2018**, *6*, 5152−5161.
(58) Karthikeyan, P.; Banu, H. A. T.; Meenakshi, S. Synthesis and characterization of metal loaded chitosan-alginate biopolymeric hybrid beads for the efficient removal of phosphate and nitrate ions from aqueous solution. *Int. J. Biol. Macromol.* **2019**, *130*, 407−418.
(59) Ionita, M.; Pandele, M. A.; Iovu, H. Sodium alginate/graphene oxide composite films with enhanced thermal and mechanical properties. *Carbohydr. Polym.* **2013**, *94*, 339−344.
(60) Chubar, N.; Gerda, V.; Megantari, O.; Mičušík, M.; Omastova, M.; Heister, K.; Man, P.; Fraissard, J. Applications versus properties of Mg-Al layered double hydroxides provided by their syntheses methods: Alkoxide and alkoxide-free sol-gel syntheses and hydro-thermal precipitation. *Chem. Eng. J.* **2013**, *234*, 284−299.
(61) Ahmed, A. A. A.; Talib, Z. A.; bin Hussein, M. Z. Thermal, optical, and dielectric properties of Zn-Al layered double hydroxide. *Appl. Clay Sci.* **2012**, *56*, 68−76.
(62) Larosa, C.; Salerno, M.; de Lima, J. S.; Meri, R. M.; da Silva, M. F.; de Carvalho, L. B.; Converti, A. Characterisation of bare and tannase-loaded calcium alginate beads by microscopic, thermogravi-metric, FTIR and XRD analyses. *Int. J. Biol. Macromol.* **2018**, *115*, 900−906.
(63) Ambrogi, V.; Fardella, G.; Grandolini, G.; Perioli, L.; Tiralti, M. C. Intercalation compounds of hydrotalcite-like anionic clays with anti-inflammatory agents, II: uptake of diclofenac for a controlled release formulation. *Aaps Pharmscitech* **2002**, *3*, 77−82.
(64) Bernardo, M. P.; Ribeiro, C. [Mg-Al]-LDH and [Zn-Al]-LDH as matrices for removal of high loadings of phosphate. *Mater. Res.* **2018**, *21*, 1−9.
(65) Rives, V. Characterisation of layered double hydroxides and their decomposition products. *Mater. Chem. Phys.* **2002**, *75*, 19−25.
(66) Bernardo, M. P.; Moreira, F. K.; Ribeiro, C. Synthesis and characterization of eco-friendly Ca-Al-LDH loaded with phosphate for agricultural applications. *Appl. Clay Sci.* **2017**, *137*, 143−150.
(67) Grishchenko, R. O.; Emelina, A. L.; Makarov, P. Y. Thermodynamic properties and thermal behavior of Friedel's salt. *Thermochim. Acta* **2013**, *570*, 74−79.
(68) de Jager, H. J.; Prinsloo, L. C. The dehydration of phosphates monitored by DSC/TGA and in situ Raman spectroscopy. *Thermochim. Acta* **2001**, *376*, 187−196.
(69) Eshaq, G.; Rabie, A. M.; Bakr, A. A.; Mady, A. H.; ElMetwally, A. E. Cr (VI) adsorption from aqueous solutions onto Mg-Zn-Al LDH and its corresponding oxide. *Desalination Water Treat.* **2016**, *57*, 20377−20387.
(70) Guo, L.; Zhang, F.; Lu, J.; Zeng, R.; Li, S.; Song, L.; Zeng, J. A comparison of corrosion inhibition of magnesium aluminum and zinc aluminum vanadate intercalated layered double hydroxides on magnesium alloys. *Front. Mater. Sci.* **2018**, *12*, 198−206.
(71) Liu, J.; Song, J.; Xiao, H.; Zhang, L.; Qin, Y.; Liu, D.; Hou, W.; Du, N. Synthesis and thermal properties of ZnAl layered double hydroxide by urea hydrolysis. *Powder Technol.* **2014**, *253*, 41−45.
(72) Bernardo, M. P.; Moreira, F. K.; Colnago, L. A.; Ribeiro, C. Physico-chemical assessment of [Mg-Al-PO4]-LDHs obtained by structural reconstruction in high concentration of phosphate. *Colloids Surf, A Physicochem Eng. Asp* **2016**, *497*, 53−62.
(73) Karthikeyan, P.; Meenakshi, S. Development of sodium alginate@ZnFe-LDHs functionalized beads: Adsorption properties and mechanistic behaviour of phosphate and nitrate ions from the aqueous environment. *Environmental Chemistry and Ecotoxicology.* **2021**, *3*, 42−50.
(74) Han, Y. U.; Lee, W. S.; Lee, C. G.; Park, S. J.; Kim, K. W.; Kim, S. B. Entrapment of Mg-Al layered double hydroxide in calcium alginate beads for phosphate removal from aqueous solution. *Desalin. Water Treat.* **2011**, *36*, 178−186.
(75) Cardoso, L. P.; Celis, R.; Cornejo, J.; Valim, J. B. Layered double hydroxides as supports for the slow release of acid herbicides. *J. Agric. Food Chem.* **2006**, *54*, 5968−5975.
(76) Silva, V. D.; Mangrich, A. S.; Wypych, F. Nitrate release from layered double hydroxides as potential slow-release fertilizers. *Rev. Bras. Cienc. Solo.* **2014**, *38*, 821−830.
(77) Solubility Product Constants near 25°C. https://www.chm.uri.edu/weuler/chm112/refmater/KspTable.html.
(78) Onishi, B. S. D.; dos Reis Ferreira, C. S.; Urbano, A.; Santos, M. J. Modified hydrotalcite for phosphorus slow-release: Kinetic and sorption-desorption processes in clayey and sandy soils from North of Paraná state (Brazil). *Appl. Clay Sci.* **2020**, *197*, 105759.
(79) Seida, Y.; Nakano, Y. Removal of phosphate by layered double hydroxides containing iron. *Water Res.* **2002**, *36*, 1306−1312.
(80) Shibata, J.; Murayama, N.; Nakajima, S. pH buffering action of layered double hydroxide. *Kagaku Kogaku Ronbunshu.* **2007**, *33*, 273−277.
(81) Borgiallo, A.; Rojas, R. Reactivity and heavy metal removal capacity of calcium alginate beads loaded with Ca-Al layered double hydroxides. *J. Chem. Eng.* **2019**, *3*, 22.
(82) Veglio, F; Esposito, A; Reverberi, A.P Copper adsorption on calcium alginate beads: equilibrium pH-related models. *Hydro-metallurgy* **2002**, *65*, 43−57.
(83) Kinoshita, T.; Yano, T.; Sugiura, M.; Nagasaki, Y. Effects of controlled-release fertilizer on leaf area index and fruit yield in high-density soilless tomato culture using low node-order pinching. *PloS one* **2014**, *9*, No. e113074.
(84) Ashekuzzaman, S.; Jiang, J. Study on the sorption-desorption-regeneration performance of Ca-, Mg-and CaMg-based layered double hydroxides for removing phosphate from water. *Chem. Eng. J.* **2014**, *246*, 97−105.

https://doi.org/10.1021/acsomega.2c07862
ACS Omega 2023, 8, 15017−15030

(85) Trientini, F.; Fisher, P. R. Hydroponic fertilizer supply for basil using controlled-release fertilizer. *HortScience* **2020**, *55*, 1683−1691.
(86) Du, C.; Zhou, J.; Shaviv, A. Release characteristics of nutrients from polymer-coated compound controlled release fertilizers. *J. Polym. Environ* **2006**, *14*, 223−230.
(87) Devau, N.; Le Cadre, E.; Hinsinger, P.; Jaillard, B.; Gérard, F. Soil pH controls the environmental availability of phosphorus: experimental and mechanistic modelling approaches. *Appl. Geochem.* **2009**, *24*, 2163−2174.
(88) Akinremi, O.; Cho, C. Phosphate Transport in Calcium-Saturated Systems: II. Experimental Results in a Model System. *Soil Sci. Soc. Am. J.* **1991**, *55*, 1282−1287.
(89) Devau, N.; Le Cadre, E.; Hinsinger, P.; Gérard, F. A mechanistic model for understanding root-induced chemical changes controlling phosphorus availability. *Ann. Bot.* **2010**, *105*, 1183−1197.

https://doi.org/10.1021/acsomega.2c07862
ACS Omega 2023, 8, 15017−15030